THE JOURNAL OF PHYSICAL CHEMISTRY C

Article

pubs.acs.org/JPCC

Electronic Structure of Low-Dimensional Carbon π-Systems

J. M. García-Lastra,[†,■] Idris Boukahil,[‡,▲] Ruimin Qiao,[§] Angel Rubio,[∥,⊥] and F. J. Himpsel*[,‡]

[†]Department of Energy Conversion and Storage, Technical University of Denmark, Fysjikvej 309, 2800 Kongens Lyngby, Denmark

[‡]Department of Physics, University of Wisconsin Madison, 1150 University Avenue, Madison, Wisconsin 53706, United States

[§]Advanced Light Source, Lawrence Berkeley National Laboratory, Berkeley, California 94720, United States

[∥]Max Planck Institute for the Structure and Dynamics of Matter, Hamburg, Germany

[⊥]Nano-Bio Spectroscopy Group and ETSF, Universidad del Pais Vasco CFM CSIC-UPV/EHU-MPC & DIPC, 20018 San Sebastian, Spain

Supporting Information

ABSTRACT: X-ray absorption spectroscopy (XAS) is combined with density functional theory (DFT) to determine the orbitals of one- and two-dimensional carbon π-systems (lycopene, beta-carotene, retinal, retinol, retinoic acid, coronene, triphenylene). Considerable fine structure is observed for the transition from the C 1s level to the lowest unoccupied molecular orbital (LUMO) and explained by DFT. The wave functions of the one-dimensional chain molecules display the node structure of a vibrating string. The XAS transition energy is decomposed into contributions from the C 1s core level, the π^* final state, and the electron−hole interaction. For the latter, we develop a simple model that accurately represents a full Δ-self-consistent field (ΔSCF) calculation. The distortion of the LUMO because of its interaction with the C 1s hole is investigated. These results illustrate the electronic states of prototypical π-bonded carbon structures with low-dimensional character, such as those used in molecular complexes for solar cells, confined graphene structures, and molecular wires.

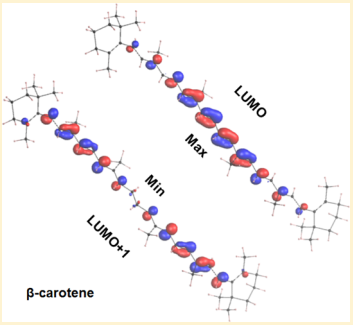

INTRODUCTION

Carbon-based electronics is on the rise. Examples are transistors based on carbon nanotubes or graphene, organic light-emitting diodes (OLEDs), solar cells containing conducting polymers or organic dye molecules, single-molecule devices, and many other innovative structures. A particularly exciting concept utilizes molecular building blocks, stitched together by molecular wires into complexes that perform sophisticated functions.[1−8] For example, dye-sensitized solar cells consisting of a donor-π-absorber (d-π-a) complex have set an efficiency record for this class of solar cells.[9] In this case, a planar π-system plays the role of the light absorber. The electronic structure of such a complex has been investigated by X-ray absorption spectroscopy (XAS),[10] taking advantage of the element and orbital selectivity of this technique. The appeal of such structures is their atomic precision, which avoids having to deal with disordered, intermixed interfaces between different materials in conventional solar cells. As a next step in this scheme, it has been proposed to connect two such absorber molecules by a molecular wire or diode into a tandem device in order to cover the solar spectrum more efficiently. Thousands of candidate molecules have been screened by density functional theory to see whether their energy levels are suitable for tandem arrangements.[11]

The building blocks in molecular electronics typically contain carbon-based π-systems with a band gap in the 1−3 eV range. These can be one-dimensional molecular wires, such as the classic *trans*-polyacetylene, or two-dimensional molecular sheets, such as pentacene. Like *trans*-polyacetylene, the one-dimensional carbon π-systems investigated here contain a single chain of π-bonded carbon atoms and thus form the finest conceivable wires. We are interested in a fundamental understanding of the π-orbitals that carry the electrons and absorb/emit photons. What determines the energies and splittings of these frontier orbitals? How can one predict the electron−hole interaction that leads to the formation of neutral excitons with a long mean free path? Does it change in low-dimensional systems?[12−14] The exciton binding energy is an important number when breaking up excitons into free carriers in organic solar cells[15] or generating light from excitons in OLEDs.[16]

This study uses prototypical π-systems to represent building blocks in molecular electronics. For one-dimensional wirelike building blocks, we choose molecules containing π-bonded carbon chains similar to *trans*-polyacetylene but with well-defined finite lengths. Lycopene has the longest carbon chain studied here, followed by beta-carotene[4−6,17,18] and the group consisting of retinal, retinol, and retinoic acid. As two-dimensional prototypes of finite-sized graphene, we select coronene,[19−21] triphenylene, and benzene[22] again descending in size. The lowest π^* orbitals of these molecules are probed by optical transitions from the C 1s core level via XAS. Such core

Received: March 10, 2016
Revised: May 6, 2016
Published: May 18, 2016

DOI: 10.1021/acs.jpcc.6b02530
J. Phys. Chem. C 2016, 120, 12362−12368

level spectra allow a unique assignment of the observed absorption peaks to specific π^* orbitals, while UV/vis absorption spectroscopy confounds transitions from several occupied π-orbitals into the π^*-system.

Despite the complexity of these molecules, we find surprisingly sharp features in the XAS spectra. Density functional theory provides a detailed analysis of the spectra in terms of π^* orbitals and their wave functions. Furthermore, the XAS transition energy is decomposed into the C 1s core level energy, the energy of the π^* level, and the electron−hole interaction. The high symmetry and the small size of these molecules reduce the number of π^* orbitals near the threshold. This allows a simple interpretation of the wave functions, particularly for the carbon chains. The envelope of the rapidly oscillating π^* orbitals simply represents the electronic analog of the overtones generated by a vibrating string.

EXPERIMENTAL METHODS

The XAS experiments were performed at an undulator beamline of the Advanced Light Source (ALS) at LBNL. The photon energy reference for these spectra was based on the π^* transition of graphite and graphene (on Cu foil), which was at 285.35 eV. The slits were kept very narrow to resolve vibrational fine structure at a level of better than 0.1 eV. This also minimized radiation damage which occurred readily for the 1D molecules studied here. Their sensitivity rivaled the most sensitive molecules encountered in our previous studies of photochemical reactions.[23,24] This is illustrated in Figure 1,

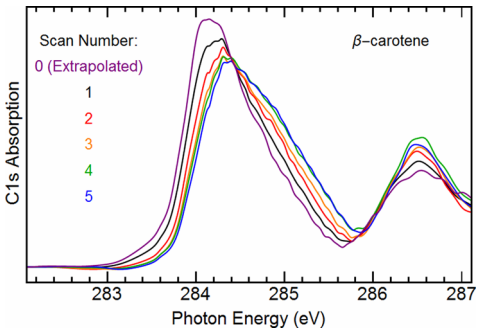

Figure 1. Effect of radiation damage on the C 1s absorption spectrum of beta-carotene. The intrinsic π^* peak at 284.2 eV is reduced while the π^* feature of graphitic carbon near 285 eV is growing. The first spectrum is extrapolated to a pristine sample by subtracting the difference between the second and the first spectrum.

where subsequent scans of the same sample area are shown for beta-carotene. In addition to nearly closing the slits, the beam was defocused to an area of about 2 × 3 mm^2, and the total electron yield mode was used for efficient detection. Despite these efforts, the characteristic π^* peak at 284.2 eV starts to fade already after the first scan in Figure 1, giving eventually way to a new feature near 285 eV (possibly because of graphitic carbon from dehydrogenation). To estimate what a completely pristine spectrum would look like, the difference between spectrum 1 and 2 was subtracted from spectrum 1. The resulting spectrum (labeled 0) represents our best estimate of a pristine spectrum.

A characteristic difficulty at the C 1s threshold is the normalization of the spectra to the true photon flux. It is reduced by carbon contamination on the optics in the region of the π^* transitions. The flux was monitored simultaneously with the sample current by the photocurrent from a Au-coated mesh in the path of the beam. Hydrocarbon contamination on the Au mesh mimics extra flux that is not there, leading to a dip after dividing the sample current by the mesh current. Therefore, we also measured clean Au samples under the same conditions. The double-division (sample/mesh)/(Au/mesh) cancels the contribution from a contaminated mesh.

The molecules were obtained as microcrystalline powders from Sigma-Aldrich and were kept refrigerated until use. They were rubbed onto double-sided Cu tape. A possible contribution from residual exposed glue on the tape was characterized by measuring the bare tape separately. The signal from the tape was low and featureless below a characteristic peak at 288.5 eV (not shown). This peak was used to determine the tape contribution and to subtract it out. In the spectral region shown in the figures, this subtraction did not influence the shape of the spectra.

THEORETICAL METHODS

Density functional theory (DFT) calculations were carried out by means of the Amsterdam Density Functional (ADF) code.[25] All atoms were described by basis sets of TZP quality (triple-ζ Slater-type orbital plus one polarization function) as provided by the program database. All core electrons were handled explicitly (without making the frozen-core approximation). The exchange-correlation energy was computed via three different exchange-correlation functionals: (1) the Vosko−Wilk−Nussair (VWN) functional[26] at the local density approximation (LDA) level, (2) the Perdew−Burke−Ernzerhof (PBE) functional[27] at the generalized gradient approximation (GGA) level, and (3) the BHandHLYP hybrid functional.[25]

The particular choice of the BHandHLYP functional among many other hybrid functionals for the time-dependent DFT (TD-DFT) calculations is based on previous work, where the BHandHLYP functional required the smallest energy shift to match the threshold of the experimental XAS spectra. At the same time, it gave the best agreement for the relative peak positions in the spectra.[28] In general, hybrid functionals with a large percentage of exact exchange, such as BHandHLYP or BHandH[25] with 50%, exhibit much smaller deviations for core-to-valence transitions than standard hybrid functionals, such as PBE0[29] or B3LYP[30] with 25% (∼1 eV vs ∼10 eV, respectively).[31]

DFT/TD-DFT has drawbacks when describing conical intersections, long-range charge transfer excitations, or double excitations.[32] These weaknesses are mainly due to the single-determinant nature of DFT. Many efforts have been made to construct new DFT/TD-DFT functionals that overcome these problems.[33] Despite these shortcomings, the DFT/TD-DFT framework is defacto the most popular technique to model XAS spectra as a result of the balance between its cost and its accuracy.[32] In parallel wave function approaches and many-body techniques have also been employed to calculate the spectra of polyenes and carotene molecules similar to the ones investigated in the present study. Examples are the density matrix renormalization group (DMRG) studies by Hachmann et al. on the radical character of acenes,[2] the low-lying excited states of polyenes and β-carotene,[3] and the benchmark study by Hajgató et al. of the ground state of polyacenes and their singlet−triplet splitting.[34] Thereby, the multideterminant complete active space self-consistent field (CASSCF) method was compared with single-determinant methods, such as Hartree−Fock, MP2, or coupled-clusters,[34] as well as with

DOI: 10.1021/acs.jpcc.6b02530
J. Phys. Chem. C 2016, 120, 12362−12368

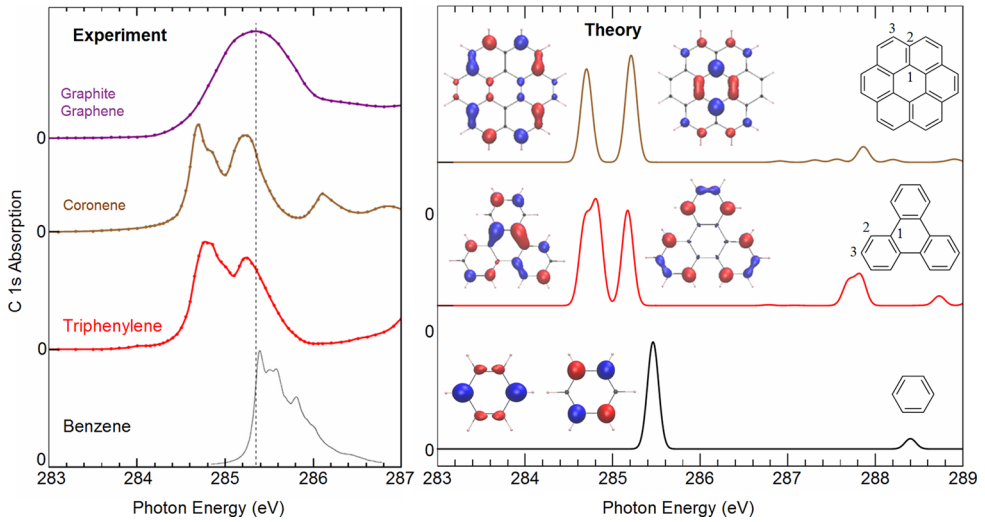

Figure 2. X-ray absorption spectra for the smallest molecules with the structure of graphene. The lowest C 1s-to-π^* transitions are compared to TD-DFT calculations. The fine structure is a combination of electronic and vibrational interactions (see the gas-phase spectrum of benzene from Ma et al.[22]). The insets show calculated wave functions of the degenerate LUMO of benzene and the split LUMOs in the larger molecules. Those contain inequivalent atoms (numbered). All theory spectra are shifted up in energy by 1.8 eV to match the data.

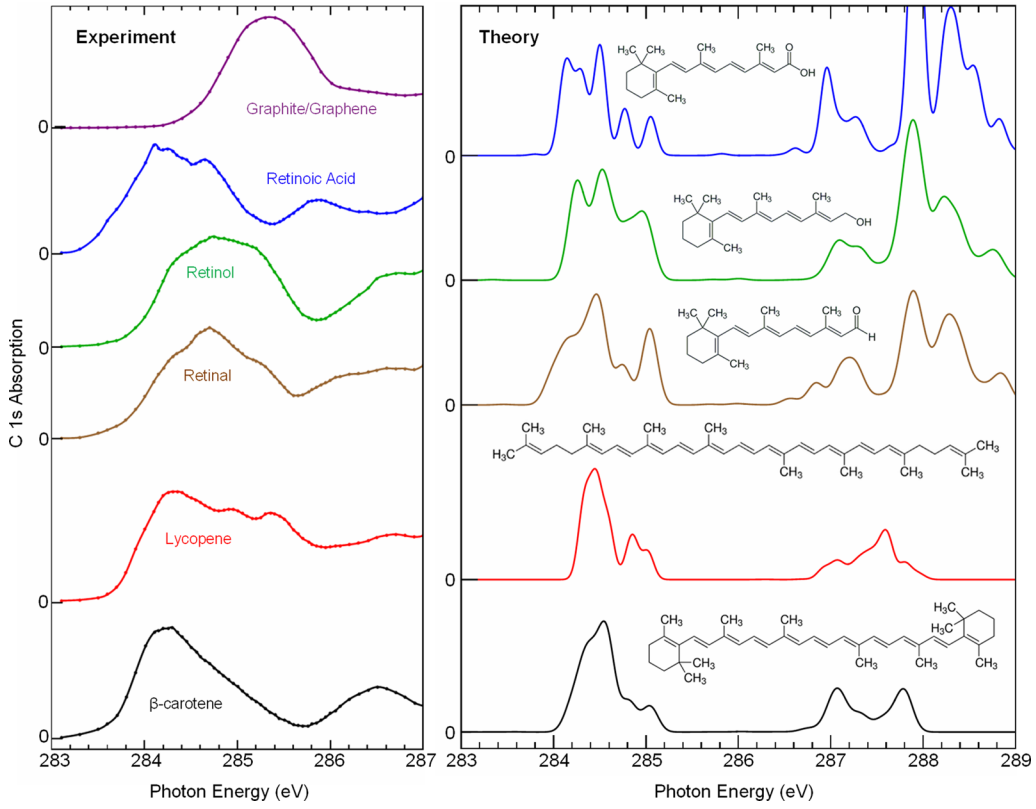

Figure 3. Experimental and calculated spectra of 1D molecular wires containing a single chain of π-bonded C atoms. The presentation of the spectra is analogous to Figure 2. The corresponding wave functions are shown in Figure 4 and in the Supporting Information.

DFT at the hybrid level from the seminal work by Bendikov et al.[1] More details about the performance of wave function methods in this kind of systems, such as DMRG or the multireference configuration interaction (MRCI) method, can be found in several reviews.[35,36] Only a small number of XAS calculations have been performed using many-body approaches because of their computational cost. An example is the recent study on small- and medium-size molecules by Wenzel and co-workers.[37,38]

The starting point of our calculations was a structure determination of the molecules in their ground state. They were relaxed until the maximum force was reduced to less than 0.04 eV/Å. Then, the XAS transitions were calculated using TD-DFT which takes the electron−hole interaction into account. Since systematic errors make it very difficult for first-principles calculations to reach an absolute accuracy of better than 1 eV for core level transitions, the theoretical spectra were shifted to match the XAS data (by the same

DOI: 10.1021/acs.jpcc.6b02530
J. Phys. Chem. C 2016, 120, 12362−12368

amount for all molecules). The BHandHLYP functional required the smallest shift (1.8 eV upward). The relative peak positions were reproduced best by this functional as well. For this reason, the BHandHLYP results were used for all figures.

It is instructive to decompose the XAS transition energy into contributions from the core level, the empty π^* orbital, and the electron−hole interaction. Such an analysis was performed for each molecule using Δ-self-consistent field (ΔSCF) calculation methodology at the LDA level.[39] In contrast to TD-DFT calculations, the ΔSCF results were nearly independent of the exchange-correlation functional for the lowest transition.[27] Therefore, we selected the core excitation that contributes most strongly to this transition. The energy of the lowest empty π^* orbital (lowest unoccupied molecular orbital, LUMO, level) involves calculating the electron affinity (EA) of a molecule using the vacuum level as reference energy. EA is obtained as the ΔSCF energy difference between the ground states of the neutral molecule and the negative ion (with the extra electron in the LUMO). In similar fashion, the energy of the C 1s core level of a particular atom in the molecule is calculated relative to the vacuum level. In this case, we used a ΔSCF calculation taking the difference between the ground states of the neutral molecule and the molecule with one electron removed from a C 1s level. The energy difference between EA and the C 1s level from ΔSCF corresponds to the quasiparticle gap between the C 1s level and the LUMO.[40] The optical gap, that is, the photon energy of the C 1s-to-LUMO transition is reduced by the electron−hole (e-h) interaction between the electron in the LUMO and the C 1s hole. It was obtained again via ΔSCF by calculating the total energy of the molecule with an electron promoted from the C 1s level to the LUMO and then by subtracting the ground-state energy. The electron−hole interaction energy is given by the difference between the quasiparticle and optical gaps. A recent determination of the e-h interaction in molecules for OLEDs also used ΔSCF calculations to obtain quasiparticle gaps but complemented them with experimental input from X-ray photoelectron spectroscopy (XPS), ultraviolet photoelectron spectroscopy (UPS), and optical absorption in the UV/vis.[16] The electron−hole interaction can also be investigated experimentally via resonant inelastic X-ray scattering (RIXS). This has been accomplished at the C 1s edge for π-bonded C60.[41]

RESULTS

XAS spectra are shown in Figure 2 for 2D molecules and in Figure 3 for 1D molecules. They are paired with calculated spectra (using TD-DFT). The respective wave functions of the lowest π^* orbitals are given in Figures 2 and 4. Compared to the graphite reference spectrum at the top of Figure 2, the molecules exhibit considerable extra fine structure. The spectrum of graphene on Cu was similar to that of graphite (not shown). The center of this peak was taken as reference energy for XAS (dashed line at 285.35 eV). A spectrum of gas-phase benzene from Ma et al. is also shown,[22] representing the smallest member in this series of 2D, snow-flake shaped molecules. On the basis of the detailed analysis of the benzene spectrum[22] (including deuterated benzene), the structured asymmetric tail is due to excitations of molecular vibrations in addition to the core excitation. The calculation predicts only a single peak from the two degenerate orbitals shown on the lower right. Vibrational excitations are not included in the calculation. They have been investigated extensively in a recent study.[21] The next π^* orbital lies about 3 eV higher and is well separated from the LUMO. The XAS spectra of triphenylene and coronene exhibit a similar sawtooth shape but with two replicas of the sawtooth. This matches the calculated spectra, which predict a split LUMO corresponding to a combination of different envelope wave functions and inequivalent C atoms (numbered in the structural drawings). Detailed results about the nature of these orbitals are given in the Supporting Information.

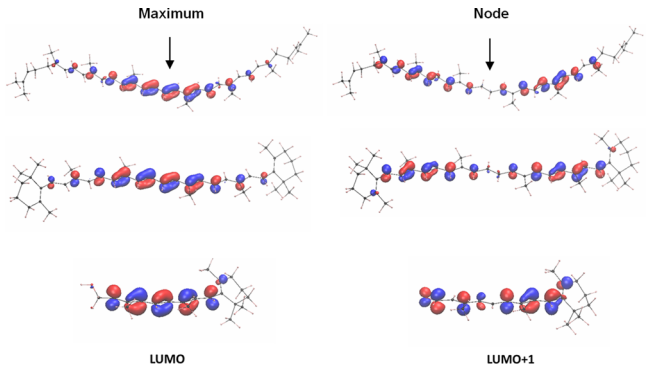

Figure 4. Calculated wave functions for the LUMO and LUMO+1 of molecules with π-bonded C chains (lycopene on top, β-carotene in the middle, and retinol at the bottom). The sign of the antibonding π^*-orbitals changes rapidly from one atom to the next (red = +, blue = −). The envelope function behaves like a vibrating string, with a maximum at the center for the LUMO and node for the LUMO+1.

The spectra of the 1D molecules containing π-bonded carbon chains are shown in Figure 3. They are more complex, reflecting the lower symmetry and the larger size of these molecules. The broader, but still structured XAS spectra indicate a more complex splitting of the unoccupied orbitals.. The calculation predicts two manifolds separated by about 3 eV, similar to the splitting of the two orbitals in benzene. Both manifolds are rather complex, containing about five dominant lines each according to the TD-DFT calculations. The decomposition is rather complex, involving contributions from a single C atom to both LUMO and LUMO+1 (see the Supporting Information for a thorough description of the contributions to each line). A comparison with the data reveals similarities between the dominant features, particularly for the simpler spectra of beta-carotene and lycopene. The intensity ratios of the main features are similar, but the experimental splittings are significantly larger. A quantitative analysis is difficult because of the vibrational structure which is comparable to the orbital splittings, judging from Figure 2.

Despite the complexity of the XAS spectra and the calculated manifolds, the 1D carbon chains can be understood using a simple model, as demonstrated in Figure 4. Thereby, we borrow the concept of an envelope function from the analysis of quantum well states.[42−44] While the wave functions of antibonding π^* orbitals oscillate rapidly from one C atom to the next, the envelope of these rapid oscillations is rather simple. The LUMO exhibits nodes in the envelope function at the ends of the C chain and a maximum at the center. The LUMO+1 contains an extra node at the center. This pattern is typical for all the 1D chain molecules investigated here. It is demonstrated in Figure 4 for three representative molecules with different lengths. Images for the remaining molecules can be found in the Supporting Information. This behavior is the quantum analog of a vibrating string which generates higher-frequency overtones when the number of nodes increases. Such

DOI: 10.1021/acs.jpcc.6b02530
J. Phys. Chem. C 2016, 120, 12362−12368

simplicity is characteristic of 1D systems. The resonance modes of a 2D drum are already much more complex, as evidenced by the intricate wave functions of triphenylene and coronene in Figure 2.

Figure 5 addresses the energetics of the C 1s-to-π^* transitions. The transition energy in the XAS spectra is

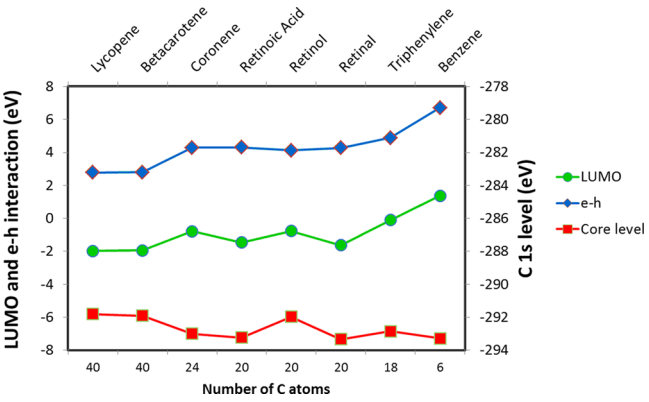

Figure 5. Decomposition of the C 1s-to-LUMO transition energy into the contributions from the core level energy, the LUMO energy, and the electron–hole (e-h) interaction. The latter is best described as a function of the molecular size (plotted along the *x*-axis). Larger molecules exhibit smaller e-h interactions, as explained by the model in eq 1 and Figure 6.

determined by three components, that is, the energy of the C 1s core level, the LUMO energy, and the e-h interaction. The C 1s-to-π^* quasiparticle gaps between the red and green curves vary over a range of 5 eV, while the optical ΔSCF gaps vary less than 1 eV (not shown). This implies that the larger quasiparticle gap for the molecules on the right side of Figure 5 is nearly compensated by a larger e-h interaction for the XAS transition energy. For instance, the quasiparticle gap is 294.67 eV for benzene and 289.83 eV for lycopene (a difference of 4.84 eV), while the optical ΔSCF gap is 287.95 eV for benzene and 287.05 eV for lycopene (a difference of 0.9 eV). The resulting e-h interaction is 6.72 eV for benzene and 2.78 eV for lycopene.

The general trend of the e-h interaction is best described by the size of the molecules, which is taken as the number of C atoms in Figure 5. Smaller molecules have larger e-h interactions. This observation can be rationalized by a simple model. The model assumes that the orbital of the excited level is evenly distributed among all the carbon atoms in the molecule. If one takes the electron–hole interaction as the monopole Coulomb interaction between the core hole and the evenly distributed excited electron, the e-h energy for the core level of atom *i* can be written in atomic units as

$$E_i^{\text{e-h}} = \frac{E^{\text{on-site}}}{n} + \frac{1}{n}\sum_{i\neq j}^{n}\frac{1}{|\vec{r}_i - \vec{r}_j|} \quad (1)$$

where $E^{\text{on-site}}$ represents the interaction between a core hole and an electron excited in the p_z orbital of the same C atom and *n* is the number of carbon atoms in the molecule. Figure 6 displays the predictions of the model to the ΔSCF results using $E^{\text{on-site}}$ = 1.2 eV. A linear approximation of the comparison for various molecules produces a high correlation R^2 = 0.98. This allows rapid estimates of the e-h interaction for core levels.

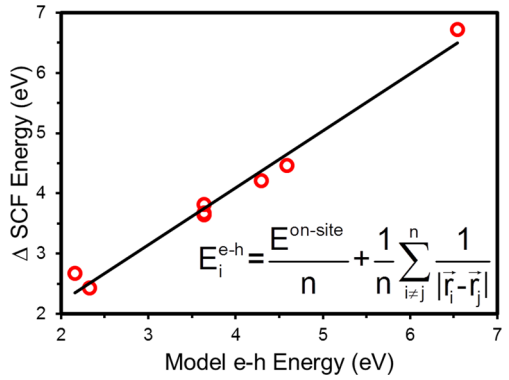

Figure 6. A simple model for the electron–hole interaction, compared to the full ΔSCF calculation. A high correlation of R^2 = 0.98 is found for the line $E_{\Delta SCF} = 0.95 \cdot E_{\text{Model}} + 0.31$ eV.

Excitons in low-dimensional systems have attracted substantial attention.[12−14] Because of the reduced number of neighbor atoms, one expects less screening of the Coulomb interaction in lower dimensions and thus a larger exciton binding energy.[45] Here, we find that the overall size of the molecule may play an even more important role. It appears that not only the immediate neighbor atoms contribute to the screening of the core hole but also the remainder of the molecule.

The e-h interaction changes not only the energetics, it also alters the wave functions and the resulting charge density. This is illustrated in Figure 7. As one can see in panel d, the core

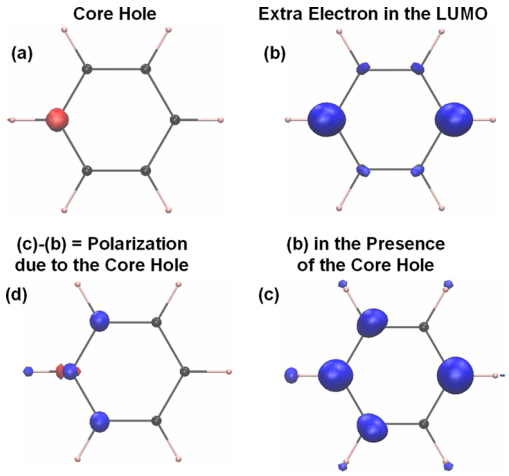

Figure 7. Effect of a C 1s core hole on the charge density of the lowest π^* orbital of benzene (clockwise from the top left). The positive charge of the core hole (red) attracts negative charge to the atom containing the core hole and its neighbors (blue). Notice that these plots are different from Figure 2, where the wave functions are shown.

hole attracts negative charge which nearly compensates its positive charge. A substantial amount of negative charge is also attracted to the adjacent C. Such a visualization of the consequences of electron–hole interaction helps in understanding the role of the core hole in XAS. This has been a major obstacle to the quantitative exploitation of XAS experiments.

DOI: 10.1021/acs.jpcc.6b02530
J. Phys. Chem. C 2016, 120, 12362−12368

CONCLUSIONS

This work systematically explores the electronic structure of prototypical one- and two-dimensional molecules containing π-bonded atom chains and sheets. The 1D chains represent short sections of *trans*-polyacetylene, while the sheets correspond to the smallest implementations of confined graphene (retaining 3-fold or 6-fold symmetry). Such structures are relevant to carbon-based electronics and optoelectronics, where they can serve as precise building blocks for multifunctional complexes, such as d-π-a or tandem solar cells. The decomposition of the XAS transition energy into the single-particle energy levels and the electron−hole interaction provides quantitative information for designing molecular complexes with optimized electronic performance.

Despite the complexity of these molecules, we find surprisingly sharp features in the XAS spectra. The high symmetry and small size limits the number of π^*-orbitals near the LUMO. This allows a simple interpretation of the wave functions, particularly for the carbon chains. The envelope of the rapidly oscillating π^*-orbitals simply represents the electronic analog of the overtones generated by a vibrating string.

ASSOCIATED CONTENT

Supporting Information

The Supporting Information is available free of charge on the ACS Publications website at DOI: 10.1021/acs.jpcc.6b02530.

1. Analysis of the main peaks in the 1D molecules (retinoic acid, retinol, retinal, lycopene, beta-carotene). 2. Analysis of the main peaks in the 2D molecules (benzene, coronene, triphenylene)
(PDF)

AUTHOR INFORMATION

Corresponding Author

*Phone: 608-263-5590; e-mail: fhimpsel@wisc.edu.

Notes

The authors declare no competing financial interest.

■Lead author for the theoretical part.

▲Lead author for the experimental part.

ACKNOWLEDGMENTS

The help of Wanli Yang with the experiment is gratefully acknowledged. This research was supported by the NSF through the University of Wisconsin Materials Research Science and Engineering Center (DMR-1121288). We also acknowledge support by the DOE (BES) for the synchrotron radiation experiments at the Advanced Light Source (ALS) under the Contracts DE-AC02-05CH11231 (ALS) and DE-SC0006931 (endstation). J.M.G.L. acknowledges support from the Spanish Ministry of Economy and Competitiveness under Projects FIS2012-30996 and FIS2013-46159-C3-1-P, Grupos Consolidados (IT578-13), and COST Action MP1306 (EUSpec).

REFERENCES

(1) Bendikov, M.; Duong, H. M.; Starkey, K.; Houk, K. N.; Carter, E. A.; Wudl, F. Oligoacenes: Theoretical Prediction of Open-Shell Singlet Diradical Ground States. *J. Am. Chem. Soc.* **2004**, *126*, 7416−7417.

(2) Hachmann, J.; Dorando, J. J.; Avilés, M.; Chan, G. K.-L. The Radical Character of the Acenes: A Density Matrix Renormalization Group Study. *J. Chem. Phys.* **2007**, *127*, 134309.

(3) Ghosh, D.; Hachmann, J.; Yanai, T.; Chan, G. K.-L. Orbital Optimization in the Density Matrix Renormalization Group, with Applications to Polyenes and β-carotene. *J. Chem. Phys.* **2008**, *128*, 144117.

(4) Spallanzani, N.; Rozzi, C. A.; Varsano, D.; Baruah, T.; Pederson, M. R.; Manghi, F.; Rubio, A. Photoexcitation of a Light-Harvesting Supramolecular Triad: A Time-Dependent DFT Study. *J. Phys. Chem. B* **2009**, *113*, 5345−5349.

(5) Liddell, P. A.; Kuciauskas, D.; Sumida, J. P.; Nash, B.; Nguyen, D.; Moore, A. L.; Moore, T. A.; Gust, D. Photoinduced Charge Separation and Charge Recombination to a Triplet State in a Carotene−Porphyrin−Fullerene Triad. *J. Am. Chem. Soc.* **1997**, *119*, 1400−1405.

(6) Andrea Rozzi, C.; Maria Falke, S.; Spallanzani, N.; Rubio, A.; Molinari, E.; Brida, D.; Maiuri, M.; Cerullo, G.; Schramm, H.; Christoffers, J.; et al. Quantum Coherence Controls the Charge Separation in a Prototypical Artificial Light-Harvesting System. *Nat. Commun.* **2013**, *4*, 1602.

(7) Riss, A.; Wickenburg, S.; Gorman, P.; Tan, L. Z.; Tsai, H.-Z.; de Oteyza, D. G.; Chen, Y.-C.; Bradley, A. J.; Ugeda, M. M.; Etkin, G.; et al. Local Electronic and Chemical Structure of Oligo-acetylene Derivatives Formed Through Radical Cyclizations at a Surface. *Nano Lett.* **2014**, *14*, 2251−2255.

(8) Vasseur, G.; Fagot-Revurat, Y.; Sicot, M.; Kierren, B.; Moreau, L.; Malterre, D.; Cardenas, L.; Galeotti, G.; Lipton-Duffin, J.; Rosei, F. Quasi One-Dimensional Band Dispersion and Surface Metallization in Long-Range Ordered Polymeric Wires. *Nat. Commun.* **2016**, *7*, 10235.

(9) Yella, A.; Lee, H.-W.; Tsao, H. N.; Yi, C.; Chandiran, A. K.; Nazeeruddin, M. K.; Diau, E. W.-G.; Yeh, C.-Y.; Zakeeruddin, S. M.; Grätzel, M. Porphyrin-Sensitized Solar Cells with Cobalt (II/III)−Based Redox Electrolyte Exceed 12% Efficiency. *Science* **2011**, *334*, 629−634.

(10) Zegkinoglou, I.; Ragoussi, M.-E.; Pemmaraju, C. D.; Johnson, P. S.; Pickup, D. F.; Ortega, J. E.; Prendergast, D.; de la Torre, G.; Himpsel, F. J. Spectroscopy of Donor−π−Acceptor Porphyrins for Dye-Sensitized Solar Cells. *J. Phys. Chem. C* **2013**, *117*, 13357−13364.

(11) Ornso, K. B.; Garcia-Lastra, J. M.; De La Torre, G.; Himpsel, F. J.; Rubio, A.; Thygesen, K. S. Design of Two-Photon Molecular Tandem Architectures for Solar Cells by Ab Initio Theory. *Chem. Sci.* **2015**, *6*, 3018−3025.

(12) Yu, Z. G.; Saxena, A.; Bishop, A. R. Excitons in Quasi-One-Dimensional Organics: Strong Correlation Approximation. *Phys. Rev. B: Condens. Matter Mater. Phys.* **1997**, *56*, 3697−3716.

(13) Spataru, C. D.; Ismail-Beigi, S.; Benedict, L. X.; Louie, S. G. Excitonic Effects and Optical Spectra of Single-Walled Carbon Nanotubes. *Phys. Rev. Lett.* **2004**, *92*, 077402.

(14) Wang, F.; Dukovic, G.; Brus, L. E.; Heinz, T. F. The Optical Resonances in Carbon Nanotubes Arise from Excitons. *Science* **2005**, *308*, 838−841.

(15) Knupfer, M. Exciton Binding Energies in Organic Semiconductors. *Appl. Phys. A: Mater. Sci. Process.* **2003**, *77*, 623−626.

(16) Johnson, P. S.; Boukahil, I.; Himpsel, F. J.; Kearns, K. L.; Kang, J. H.; Lin, J.-C.; Leugers, A.; Meyers, G.; Mukhopadhyay, S.; Jackson, D. H. K.; et al. Multitechnique Approach for Determining Energy Levels and Exciton Binding Energies of Molecules for Organic Electronics. *J. Phys. Chem. C* **2016**, *120*, 1366−1374.

(17) Beck, M.; Stiel, H.; Leupold, D.; Winter, B.; Pop, D.; Vogt, U.; Spitz, C. Evaluation of the Energetic Position of the Lowest Excited Singlet State of β-carotene by NEXAFS and Photoemission Spectroscopy. *Biochim. Biophys. Acta, Bioenerg.* **2001**, *1506*, 260−267.

(18) Farrokhpour, H.; Ghandehari, M. Photoelectron Spectra of Some Important Biological Molecules: Symmetry-Adapted-Cluster Configuration Interaction Study. *J. Phys. Chem. B* **2013**, *117*, 6027−6041.

(19) Kosugi, T.; Miyake, T.; Ishibashi, S.; Arita, R.; Aoki, H. *Ab initio* Electronic Structure of Solid Coronene: Differences From and Commonalities to Picene. *Phys. Rev. B: Condens. Matter Mater. Phys.* **2011**, *84*, 020507.

DOI: 10.1021/acs.jpcc.6b02530
J. Phys. Chem. C 2016, 120, 12362−12368

(20) Wießner, M.; Lastra, N. S. R.; Ziroff, J.; Forster, F.; Puschnig, P.; Dössel, L.; Müllen, K.; Schöll, A.; Reinert, F. Different Views on the Electronic Structure of Nanoscale Graphene: Aromatic Molecule Versus Quantum Dot. *New J. Phys.* **2012**, *14*, 113008.
(21) Fronzoni, G.; Baseggio, O.; Stener, M.; Hua, W.; Tian, G.; Luo, Y.; Apicella, B.; Alfé, M.; de Simone, M.; Kivimäki, A.; et al. Vibrationally Resolved High-Resolution NEXAFS and XPS Spectra of Phenanthrene and Coronene. *J. Chem. Phys.* **2014**, *141*, 044313.
(22) Ma, Y.; Sette, F.; Meigs, G.; Modesti, S.; Chen, C. T. Breaking of Ground-State Symmetry in Core-Excited Ethylene and Benzene. *Phys. Rev. Lett.* **1989**, *63*, 2044−2047.
(23) Cook, P. L.; Johnson, P. S.; Liu, X.; Chin, A.-L.; Himpsel, F. J. Radiation Damage in Biomimetic Dye Molecules for Solar Cells. *J. Chem. Phys.* **2009**, *131*, 214702.
(24) Johnson, P. S.; Cook, P. L.; Liu, X.; Yang, W.; Bai, Y.; Abbott, N. L.; Himpsel, F. J. Universal Mechanism for Breaking Amide Bonds by Ionizing Radiation. *J. Chem. Phys.* **2011**, *135*, 044702.
(25) te Velde, G.; Bickelhaupt, F. M.; Baerends, E. J.; Fonseca Guerra, C.; van Gisbergen, S. J. A.; Snijders, J. G.; Ziegler, T. Chemistry with ADF. *J. Comput. Chem.* **2001**, *22*, 931−967.
(26) Vosko, S. H.; Wilk, L.; Nusair, M. Accurate Spin-Dependent Electron Liquid Correlation Energies for Local Spin Density Calculations: A Critical Analysis. *Can. J. Phys.* **1980**, *58*, 1200−1211.
(27) Perdew, J. P.; Burke, K.; Ernzerhof, M. Generalized Gradient Approximation Made Simple. *Phys. Rev. Lett.* **1996**, *77*, 3865−3868.
(28) Schmidt, N.; Fink, R.; Hieringer, W. Assignment of Near-Edge X-ray Absorption Fine Structure Spectra of Metalloporphyrins by Means of Time-dependent Density-Functional Calculations. *J. Chem. Phys.* **2010**, *133*, 054703.
(29) Adamo, C.; Barone, V. Toward Reliable Density Functional Methods Without Adjustable Parameters: The PBE0 model. *J. Chem. Phys.* **1999**, *110*, 6158−6170.
(30) Stephens, P. J.; Devlin, F. J.; Chabalowski, C. F.; Frisch, M. J. Ab Initio Calculation of Vibrational Absorption and Circular Dichroism Spectra Using Density Functional Force Fields. *J. Phys. Chem.* **1994**, *98*, 11623−11627.
(31) Besley, N. A.; Asmuruf, F. A. Time-dependent Density Functional Theory Calculations of the Spectroscopy of Core Electrons. *Phys. Chem. Chem. Phys.* **2010**, *12*, 12024−12039.
(32) Zhang, Y.; Hua, W.; Bennett, K.; Mukamel, S. Nonlinear Spectroscopy of Core and Valence Excitations Using Short X-Ray Pulses: Simulation Challenges. In *Density-Functional Methods for Excited States*; Ferré, N., Filatov, M., Huix-Rotllant, M., Eds.; Springer International Publishing: Cham, Switzerland, 2016; pp 273−345.
(33) Stein, T.; Kronik, L.; Baer, R. Reliable Prediction of Charge Transfer Excitations in Molecular Complexes Using Time-Dependent Density Functional Theory. *J. Am. Chem. Soc.* **2009**, *131*, 2818−2820.
(34) Hajgató, B.; Szieberth, D.; Geerlings, P.; De Proft, F.; Deleuze, M. S. A Benchmark Theoretical Study of the Electronic Ground State and of the Singlet-Triplet Split of Benzene and Linear Acenes. *J. Chem. Phys.* **2009**, *131*, 224321.
(35) Chan, G. K.-L.; Sharma, S. The Density Matrix Renormalization Group in Quantum Chemistry. *Annu. Rev. Phys. Chem.* **2011**, *62*, 465−481.
(36) Szalay, P. G.; Müller, T.; Gidofalvi, G.; Lischka, H.; Shepard, R. Multiconfiguration Self-Consistent Field and Multireference Configuration Interaction Methods and Applications. *Chem. Rev.* **2012**, *112*, 108−181.
(37) Wenzel, J.; Wormit, M.; Dreuw, A. Calculating Core-Level Excitations and X-ray Absorption Spectra of Medium-Sized Closed-Shell Molecules with the Algebraic-Diagrammatic Construction Scheme for the Polarization Propagator. *J. Comput. Chem.* **2014**, *35*, 1900−1915.
(38) Wenzel, J.; Dreuw, A. Physical Properties, Exciton Analysis, and Visualization of Core-Excited States: An Intermediate State Representation Approach. *J. Chem. Theory Comput.* **2016**, *12*, 1314−1330.
(39) García-Lastra, J. M.; Cook, P. L.; Himpsel, F. J.; Rubio, A. Communication: Systematic Shifts of the Lowest Unoccupied Molecular Orbital Peak in X-ray Absorption for a Series of 3d Metal Porphyrins. *J. Chem. Phys.* **2010**, *133*, 151103.
(40) Onida, G.; Reining, L.; Rubio, A. Electronic Excitations: Density-Functional Versus Many-Body Green's-Function Approaches. *Rev. Mod. Phys.* **2002**, *74*, 601−659.
(41) Weinhardt, L.; Fuchs, O.; Batchelor, D.; Bär, M.; Blum, M.; Denlinger, J. D.; Yang, W.; Schöll, A.; Reinert, F.; Umbach, E.; et al. Electron-hole Correlation Effects in Core-Level Spectroscopy Probed by the Resonant Inelastic Soft X-ray Scattering Map of C60. *J. Chem. Phys.* **2011**, *135*, 104705.
(42) Bastard, G. *Wave Mechanics Applied to Semiconductor Heterostructures*; Les Editions de Physique: Les Ulis Cedex, France, 1988.
(43) Ortega, J. E.; Himpsel, F. J.; Mankey, G. J.; Willis, R. F. Quantum-Well States and Magnetic Coupling Between Ferromagnets Through a Noble-Metal Layer. *Phys. Rev. B: Condens. Matter Mater. Phys.* **1993**, *47*, 1540−1552.
(44) Kawakami, R. K.; Rotenberg, E.; Choi, H. J.; Escorcia-Aparicio, E. J.; Bowen, M. O.; Wolfe, J. H.; Arenholz, E.; Zhang, Z. D.; Smith, N. V.; Qiu, Z. Q. Quantum-Well States in Copper Thin Films. *Nature* **1999**, *398*, 132−134.
(45) Frank, K. H.; Yannoulis, P.; Dudde, R.; Koch, E. E. Unoccupied Molecular Orbitals of Aromatic Hydrocarbons Adsorbed on Ag(111). *J. Chem. Phys.* **1988**, *89*, 7569−7576.

DOI: 10.1021/acs.jpcc.6b02530
J. Phys. Chem. C 2016, 120, 12362−12368